2015

Development and Implementation of a Remote-Sensing and In-situ Data Assimilating Version of CMAQ for Operational $PM_{2.5}$ Forecasting Part 1: MODIS Aerosol Optical Depth (AOD) Data-Assimilation Design and Testing

John N. McHenry
Baron Advanced Meteorological Systems, Raleigh, NC

Jeffery M. Vukovich
Baron Advanced Meteorological Systems, Raleigh, NC

N. Christina Hsu
NASA/Goddard Space Flight Center, Greenbelt, MD

Journal of the Air & Waste Management Association

ISSN: 1096-2247 (Print) 2162-2906 (Online) Journal homepage: http://www.tandfonline.com/loi/uawm20

Development and Implementation of a Remote-Sensing and In-situ Data Assimilating Version of CMAQ for Operational $PM_{2.5}$ Forecasting Part 1: MODIS Aerosol Optical Depth (AOD) Data-Assimilation Design and Testing

John N. McHenry, Jeffery M. Vukovich & N. Christina Hsu

To cite this article: John N. McHenry, Jeffery M. Vukovich & N. Christina Hsu (2015): Development and Implementation of a Remote-Sensing and In-situ Data Assimilating Version of CMAQ for Operational $PM_{2.5}$ Forecasting Part 1: MODIS Aerosol Optical Depth (AOD) Data-Assimilation Design and Testing, Journal of the Air & Waste Management Association, DOI: 10.1080/10962247.2015.1096862

To link to this article: http://dx.doi.org/10.1080/10962247.2015.1096862

Accepted author version posted online: 30 Sep 2015.

Development and Implementation of a Remote-Sensing and In-situ Data Assimilating Version of CMAQ for Operational $PM_{2.5}$ Forecasting Part 1: MODIS Aerosol Optical Depth (AOD) Data-Assimilation Design and Testing

John N. McHenry and Jeffery M. Vukovich

Baron Advanced Meteorological Systems, Raleigh, NC

N. Christina Hsu

NASA/Goddard Space Flight Center, Greenbelt, MD

Implication Statement

Air quality forecasts are now routinely used to understand when air pollution may reach unhealthy levels. For the first time, an operational air quality forecast model that includes the assimilation of remotely-sensed aerosol optical depth and ground based $PM_{2.5}$ observations is being used. The assimilation enables quantifiable improvements in model forecast skill, which improves confidence in the accuracy of the officially-issued forecasts. This helps air quality stakeholders be more effective in taking mitigating actions (reducing power consumption, ride-sharing, etc.) and avoiding exposures that could otherwise result in more serious air quality episodes or more deleterious health effects.

ABOUT THE AUTHORS

John McHenry is Chief Scientist at Baron Advanced Meteorological Systems (BAMS), a division of Baron Weather Services with principal business in Huntsville, Alabama. Jeff

Vukovich is a Senior Environmental Modeler, also at BAMS. N. Christina Hsu is the Suomi National Polar-orbiting Partnership (Suomi-NPP) Deputy Project Scientist in the Climate and Radiation Laboratory at NASA/Goddard Space Flight Center in Greenbelt, MD.

INTRODUCTION

Decision support systems for air quality planning and evaluation have been in place in the United States for nearly 40-years. Spurred by the original Clean Air Act of 1970, the identification of "criteria" pollutants (ground level ozone, particulate matter, carbon monoxide, nitrogen oxides, sulfur dioxide, and lead) created the need for air chemistry models that would help decision makers construct policy to improve public health. Initially, the 1970's saw the development of a number of such "first-generation" offline simulation models. By the 1980's, "second-generation" models were utilized by the US Environmental Protection Agency (EPA) to address pressing issues: (1) the two-layer Regional Oxidant Model (ROM) was being applied to develop ozone control strategies for the NE US Corridor; (2) the Urban Airshed Model (UAM) was being used for similar purposes at urban scales within "confined" locations such as Los Angeles; and (3) the newer Regional Acid Deposition Model (RADM) was developed and deployed as part of an integrated assessment to reduce the effects of sulfuric acid deposition (e.g. McHenry, et al.,1992). All of these air chemistry models were driven offline in retrospective simulation mode. Each used a different vertical layer structure and approach to account for the effect of meteorology on the transport, transformation, and fate of the targeted pollutants. Further, development of emissions inputs to the models was both disparate and complex. Large resource

expenditures were required to collect, process, quality control, archive, and distribute emissions inventories that the models could then read and use.

With the advent of ever increasing computational speed and the legacy of the second generation models, EPA embarked on a third generation system that would integrate the ability to represent all the criteria pollutants (except lead) within a single modeling framework (Models-3). The first prototype was the Multiscale Air Quality Simulation Platform (MAQSIP, Mathur et al., 2005). It was then replaced with what is now EPA's current-generation system, the Community Multi-Scale Air Quality (CMAQ) Model (Byun and Ching, 1999).

Despite these advancements, it was not clear that Eulerian chemistry-transport computer models (CTMs) could play a role in providing *prognostic* guidance to alert officials and the public about *real-time* air quality threats. Historically the National Weather Service had issued "Total Suspended Particulate (TSP)" forecasts (circa 1970s/1980s), but largely on their own, state agencies in the 1990s developed statistically based (regression) ozone models. The agencies did this in part to obtain forecast outlooks (1-2 day lead time) with the hope that local real-time mitigation efforts (reduced driving, lawn-mowing, air conditioning use; ride-sharing etc.) could be effective enough to avoid ozone air quality violations – too many of which could trigger automatic and expensive State Implementation Plans (SIPs) required to meet federal standards.

While these developments set the stage for CTMs to be applied in forecast mode, there were many hurdles to overcome. First, there was a certain institutional resistance to the idea at both federal and state levels. Second, to attain status as a useful tool, the ability to run a tripartite (numerical weather prediction, emissions, air chemistry) Eulerian air quality forecast decision

support system (AQF-DSS) would not only have to be demonstrated as practical (by meeting real-world forecast deadlines), but the ability to achieve results on par with locally developed statistical models and expert human air quality forecasters would also have to be shown. In the US, these accomplishments were met in a series of projects and papers beginning in the late 1990's (McHenry et al., 1999, 2000, 2001, 2004). Alongside other efforts at NCAR and NOAA/ARL (McKeen et al., 2005; Eder et al., 2005), this success helped encourage NOAA to begin investing in a National Air Quality Forecast capability beginning in FY 2000-2001 which continues to the present (Lee et al., 2012; Stajner et al., 2012). Zhang et al., 2012a,b, provide a recent comprehensive overview of the history, status, state-of-science, and future prospects of real-time/operational air quality forecasting.

In the case of the lead author, his early contributions resulted in a subscription business providing prognostic AQF-DSS ozone-only decision support to state, local, and federal agencies (such as DOE). At the same time, fine-particulate health effects became better understood and $PM_{2.5}$ standards came into effect. Thus, interest in expanding AQF capabilities to include particles was growing. In 2006, the lead author's institution, Baron Advanced Meteorological Systems (BAMS), a subsidiary of http://www.baronweather.com, implemented the first available CMAQ-based $PM_{2.5}$ forecasts to its client base. Concurrently, evaluations of offline CMAQ runs against both in-situ and remotely-sensed particle and aerosol-optical thickness data also emerged (McKeen et al. 2007; Roy et al., 2007). These studies showed that CMAQ particle deficiencies (especially in smoke, dust, secondary organics, and nitrates) could potentially benefit from remotely-sensed data-assimilation (DA). They also showed that improved science process sub-models, including better emissions, were needed (Morris et al., 2006).

This two-part paper reports on the development and implementation of a version of the CMAQ model that operationally assimilates real-time remotely-sensed aerosol optical depth (AOD) information and ground-based EPA-AirNow (http://www.airnow.gov) $PM_{2.5}$ monitor data. In Part 1 herein, the offline design and testing of the approach used to assimilate Collection 5 AOD data from the Moderate Resolution Imaging Spectroradiometer (MODIS) instruments flying on NASA's Terra and Aqua satellites is described. Aqua is part of NASA's "A-Train" (http://atrain.nasa.gov) of polar orbiter satellites with an overpass of about 1030 local solar time. Terra's overpass time is later in the day, around 1330 local solar time. By combining the differing time and space "windows" of the two satellites, a more complete picture of each daylight period's total column aerosol loading can be obtained. In the assimilation scheme, the AOD data serve as a surrogate for observed total column particulate concentrations. In Part 2 of the paper, operational implementation including the addition of real-time surface $PM_{2.5}$ monitoring data to improve the assimilation and an initial evaluation of the modeling system across the continental United States (CONUS) is presented.

BACKGROUND

A number of previous and contemporary studies have developed and tested methods to assimilate MODIS AOD and/or surface $PM_{2.5}$ data into atmospheric chemistry models, including CMAQ. Park et al., 2011 describe the assimilation of MODIS AOD data into CMAQ using an optimal interpolation (OI) method, whereby a number of free parameters establish both the model background and observational error covariance matrices. To compute the model background, CMAQ particle concentrations are converted to aerosol optical depth using a

parameterization—with small modifications--described in Malm and Hand, 2007. The authors note that Mie theory could be have been used, but that time-invariant log-normal size distribution assumptions and uncertainties in particle mixing states in CMAQ lead to large uncertainties in Mie-estimated CMAQ AODs.

More recently, Tang et al., 2015, in support of NOAA's National Center for Environmental Prediction (NCEP) National Air Quality Forecast System (Davidson, et. al., 2008), also implement an optimal interpolation (OI) approach to test MODIS AOD data assimilation in CMAQ. For meteorological inputs, they used the Weather Research and Forecasting Advanced Research WRF (WRF-ARW) model (Skamarock and Klemp, 2007) with emissions borrowed from archived real-time results at NCEP. They found that using frequent daytime assimilation updates produced the most improvement upon hourly evaluation for the 24-hour test period studied during July of 2011. Overall, model $PM_{2.5}$ biases were reduced significantly. However correlation coefficients calculated against the $PM_{2.5}$ measurements were still relatively low (at or below r=0.4; see Table 4 in Tang et al., 2015). Curiously, they did not use the same meteorological model driver that is used operationally at NCEP (WRF-NMM, see Pan et al., 2012), and only conducted the numerical experiment for a single day.

Additionally, several different approaches using the Weather Research and Forecasting Chemistry model (WRF-CHEM; Grell et al., 2005) have been explored. Using MODIS AOD data alone, Liu et al., 2011 implemented a three-dimensional variational data-assimilation (3DVAR) method based on the NCEP Gridpoint Statistical Interpolation system (GSI, Wu et al., 2002; Kleist et al., 2009) applied to the Goddard Chemistry Aerosol Radiation and Transport

(GOCART, Chin et al., 2002) module within WRF-CHEM. Their results yielded a modest improvement of surface PM_{10} forecasts when tested on a dust storm case in Asia, but no attempt was made to study the impact on surface $PM_{2.5}$. They suggested additional benefit might be gained by simultaneously assimilating surface PM_{10} data. Schwartz et al., 2012 extended this work by augmenting the WRF-CHEM GSI system to synergistically assimilate both surface $PM_{2.5}$ measurements and MODIS-derived AOD over the CONUS. They concluded that the simultaneous assimilation of both datasets produced the most improvement vis-à-vis the non-assimilating WRF-CHEM simulations. Pagowski and Grell, 2012 compared the performance of this system with another DA approach using an ensemble square-root Kalman filter (EnSRF; Whitaker and Hamill, 2002). Their intent was to explore the value, if any, of applying flow-dependent background error-covariances (BECs) versus the climatologically derived BECs used in the 3DVAR algorithm (Schwartz et al., 2012). They showed that while the EnSRF provides a small but reliable improvement over 3DVAR due to flow-dependence, their ensemble spread was too small, indicating an underestimate of the flow-dependent model error. A significant source of concern was the restriction that the GOCART module does not contain gas-phase chemistry. CMAQ, however, does represent gas-phase chemistry and includes gas-particle interactions (Binkowski and Roselle, 2003). Recently the WRF-CHEM-GOCART 3DVAR system has been updated for GSI Version 3.2 and WRF-CHEM version 4.3.1, and is now available for community application (Pagowski, et. al, 2014).

In distinction to the above, the present work relies heavily on the variational assimilation formalism and MODIS AOD data quality processing used within the operational Naval Aerosol Analysis and Prediction System (NAAPS, Zhang et al, 2008; Zhang and Reid, 2006; Hyer et al.,

2011, Daley and Barker, 2001). However, it comprises a fully independent and unique implementation configured for CMAQ. As opposed to optimal interpolation, this method uses a variational approach, in this case two-dimensional (2DVAR), exploiting the fact that the AOD is the vertical integral of the aerosol extinction coefficient. Furthermore, it differs from other reported CMAQ assimilation methods in that the assimilation is done in the state-space of the observations (Cohn et al., 1998). Moreover, as compared to NAAPS which represents only sulfur, dust, biomass-burning smoke and sea-salt, CMAQ contains a much more complete process-representation of photochemical/particle evolution, interaction, and fate (Binkowski and Roselle, 2003). Furthermore, we implement the assimilation using aerosol optical depth retrievals from both "Dark Target" (hereafter DT; Levy et al., 2007) and ─ for the first time ─ the newer "Deep Blue" (hereafter DB; Hsu et al., 2004) methods, expanding the density of remotely-sensed observations available for assimilation. This overall approach was chosen because the assimilation method had precedent in the operational community (NAAPS), yet appeared adaptable to a more complex model like CMAQ targeted for real-time prognostic application while at the same time utilizing a broader range of MODIS AOD retrievals (DT and DB). In that sense, our work represents a novel and efficient approach that should contribute to our overall understanding of the value of assimilating AOD data in complex state-of-science models like CMAQ being used within AQF-DSSs.

The offline design and testing work was conducted in partnership with NASA and the Visibility Improvement State and Tribal Association of the Southeast (VISTAS) regional planning organization (RPO). NASA was responsible for improving and providing the MODIS AOD real-time and retrospective data, and also supplied archived AERONET sun-photometer data

(http://aeronet.gsfc.nasa.gov). VISTAS provided the initial CMAQ test case consisting of its 2002 baseline annual CMAQ run, as well as its model performance evaluation (MPE, Morris et al, 2009). The MPE was invaluable in both informing the project and assuring that the author's implementation of the modeling system, including meteorology and emissions, reproduced the baseline results published by VISTAS. From this vetted baseline, changes could be made to CMAQ that would allow assessment of the impact of the assimilated AOD data against the baseline CMAQ annual run.

DEVELOPMENT OF CMAQ MODEL MODIS-AOD DATA-ASSIMILATION MODULE

Baseline CMAQ Model Version

As noted in Morris et al., 2009, VISTAS adopted the Version 4.5 release of the CMAQ model to support regional haze planning. Relatively early in the effort, VISTAS found that this version significantly under-represented concentrations of secondary organic aerosols (SOAs). Three processes, having to do with polymerization, sesqsquiterpenes, and isoprene formation were added to the model, resulting in improved SOA performance (Morris et al., 2006). This revised version, "CMAQ V4.5_soamods," was then used by VISTAS for its subsequent regional haze analysis. A slightly newer version of the model, V4.51, with the identical SOA modifications was used herein to reproduce the full 36km CONUS VISTAS 2002 annual baseline. Differences between BAMS' re-run and the original VISTAS baseline were negligible, providing confidence

that BAMS had correctly implemented the SOA-improved model and its driving meteorology and emissions. At that time, BAMS also updated its operational CMAQ model to version V4.51_soamods. This remains the current real-time forecast version that assimilates MODIS AOD data, and will be referred to simply as CMAQ or CMAQ-DA below.

AOD Data Assimilation Module

Because MODIS-observed aerosol optical depth represents an atmospheric column integral, the kernel for assimilating such data can be formulated in two dimensions absent any other source of vertical discrimination of the observations. While approaches were developed that could provide additional vertical information based on the "A-Train" satellite constellation (Jeong and Hsu, 2008), these were not available with the real-time reliability needed for the operational model. Following Zhang et al., 2008 and Cohn et al., 1998, the implemented 2-dimensional-variational (2DVAR) data-assimilation algorithm takes the following form:

$$\mathbf{T}_{b\lambda} = \mathbf{H}_{mt}(C_m) + \varepsilon_{b\lambda} \quad (1)$$

$$\mathbf{T}_{a\lambda} = \mathbf{T}_{b\lambda} + P_b\mathbf{H}^T[\mathbf{H}P_b\mathbf{H}^T + R_0]^{-1}[\mathbf{T}_{0\lambda} - \mathbf{H}(\mathbf{T}_{b\lambda})] \quad (2)$$

$$C_m = \mathbf{H}_{tm}(\mathbf{T}_{a\lambda}) + \varepsilon_m \quad (3)$$

The first equation represents the forward operator (also known as the forward model or observation operator) which takes model state variable output – concentrations of all aerosol species contributing to light reduction – and produces CMAQ's best estimate of the AOD for each grid column. This is called the model background, or $\mathbf{T}_{b\lambda}$. The second equation states that

the updated AOD analysis $\mathbf{T}_{a\lambda}$ is the "best-fit" (in a least-squares sense) combination of the model background AOD plus a correction term times the difference between the model background and the observations at the observation locations. Once an updated analysis is obtained, the third equation is applied, which inverts the updated aerosol optical depth to obtain updated model mass concentrations. More details on the implementation of each step in this process follow.

Forward Operator

In order to construct an "AOD forward operator," the project considered three light extinction algorithms. These included a parameterized Mie scheme available with CMAQ (Binkowski and Roselle, 2003), the original Interagency Monitoring of PROtected Visual Environments (IMPROVE) reconstructed mass-extinction method (RM method, following Malm et al., 1994), and a revised version of the IMPROVE RM method (Pitchford et al., 2007). Pitchford et al., 2007 showed that the revised version better replicated nephelometer data at 21 rural IMPROVE monitoring sites, especially through reducing the bias (as compared to the original method) at the high and low extremes. This effect was most apparent for the hazier eastern sites with less difference being noted in the generally clearer west. Based on these improvements, VISTAS adopted the revised parameterization and applied it to CMAQ outputs ranging from the 2002 baseline to projected-emissions-year 2018 (Morris et al., 2009). While we considered adopting the CMAQ-available Mie parameterization, and recognize that a number of AOD data-assimilation studies (e.g. Liu et al, 2011 and related) utilize Mie theory as a kernel for the

forward model, many other studies use approaches based on the original (Roy et al., 2007; Tang et al. 2015) or newer IMPROVE RM methods (Park et al., 2011; Sousan et al., 2011).

Using all viable model versus observation pairs from the 2002 annual baseline rerun, Figure 1 shows CMAQ AOD calculated using both (a) original and (b) revised IMPROVE methods against a complete set of 2002 AERONET AOD surface observations. Consistent with Pitchford et al., 2007, the figure reveals an "improvement" in the slope of the best fit line when using the revised method. This is not a true model improvement, but simply reflects improvement in the bias at both low and high extremes in revised versus original RM methods. The online Mie parameterization was also applied to the 2002 CMAQ baseline run, but it produced considerably more scatter against the AERONET observations (not shown), consistent with the previous discussion about Mie method uncertainties (Park et al., 2011). Given that VISTAS adopted the revised approach, our adoption thereof facilitated direct comparison with VISTAS results while also being consistent with the findings and approach being used by various other authors as noted above.

Figure 1 here

The revised RM method for extinction-efficiencies (b_{ext}) in 10.0 Megameter-1 is piece-wise linear and is expressed below, where sulfate, nitrate, and organic carbon are split into two fractions, representing small and large size distributions of those fractions, and aerosol concentrations are expressed in ug/m^3:

$$b_{Sulfate} = 2.2 \times f_s(RH) \times [\text{Small Sulfate}] + 4.8 \times f_l(RH) \times [\text{Large Sulfate}] \quad (4)$$

$b_{Nitrate} = 2.2 \times f_s(RH) \times [\text{Small Nitrate}] + 4.8 \times f_l(RH) \times [\text{Large Nitrate}]$ (5)

$b_{EC} = 10.0 \times [\text{Elemental Carbon}]$ (6)

$b_{OCM} = 2.8 \times [\text{Small Organic Mass}] + 6.1 \times [\text{Large Organic Mass}]$ (7)

$b_{Soil} = 1.0 \times [\text{Fine Soil}]$ (8)

$b_{CM} = 0.6 \times [\text{Coarse Mass}]$ (9)

$b_{NaCl} = 1.7 \times f_{ss}(RH) \times [\text{Sea Salt}]$ (10)

$b_{NO2} = 0.33 \times [NO_2 \text{ (ppb)}]$ (11)

Details on the apportionment of sulfate, nitrate, and total organic mass into small and large size fractions, as well as hygroscopic growth factors for small, large, and sea-salt particles are available in Pitchford et al., 2007 and IMPROVE, 2007. In our implementation, we built both online and offline (post-processing) versions of the revised RM scheme to evaluate archived model runs as well as to handle online applications, particularly real-time forecasting. Because of the highly-transient nature of NO_2 and because the MODIS AOD retrieval algorithms do not account for light extinction due to NO_2 (Levy et al., 2010), we calculate CMAQ AOD, implement the 2DVAR equations, and quantify improvements due to MODIS AOD assimilation without the NO_2 term throughout. In the above, the total extinction coefficient is the sum over all the individual species' extinction efficiencies, and the aerosol optical depth ***Tau*** is calculated as the total coefficient vertically integrated over the entire CMAQ column. Noting the improvement in CMAQ-calculated AOD gained as a result of the SOA modifications, along with the "apparent

improvement" when the revised RM scheme is used, there is still a CMAQ low-bias in AOD as compared to the AERONET observations (Figure 1, b). This model bias in the baseline VISTAS case results from underestimation of some of the CMAQ aerosol concentration fields as noted in the VISTAS model-performance evaluation.

Assimilation Step

The assimilation step is represented by equation (2). Software for this step was designed, tested and implemented following the observation-space formulation described fully in Zhang et al., 2008 and Daly and Barker, 2001. In order to obtain the least-squares best fit (or most likely) result indicated by equation (2), errors for both MODIS AOD observations and CMAQ calculated AOD's should ideally be Gaussian and un-biased. In reality, this may be more or less true depending upon the type of observation or their process representations in the atmospheric chemistry model. Clearly there is evidence that some CMAQ species (dust, wintertime nitrates, smoke, etc.) were systematically underrepresented in the 2002 results. External independent comparison of MODIS, CMAQ, and surface AERONET AOD results for summer 2001 also showed that both modeled AOD and average tropospheric mass concentrations are underestimated relative to the MODIS retrievals (Roy et al., 2007). However, these biases may be largely due to problems with external forcing (emissions) and not internal to the model itself, especially after implementing better SOA science. Schwartz et al., 2012 provide an excellent discussion of the ongoing problems with emissions inputs vis-à-vis the data-assimilation experiments they have conducted.

As noted in Zhang et al., 2008, significant care is required in pre-processing MODIS observations to produce an assimilation ready dataset. Poor quality data can ruin even the most well-intentioned data assimilation system. Further, retrievals over land and over ocean are marked by different issues and thus require different quality control procedures. For our system, the entire suite of Dark Target (DT) over-ocean and over-land quality assurance checks as fully described in Zhang and Reid, 2006 and Hyer et al., 2011 was independently implemented for application to CMAQ's 36km grid spacing (as opposed to the 1.0x1.0 degree global grid spacing of the NAAPS). Because the system also includes the relatively new Deep Blue (DB) method, in the absence of a robust error analysis the following was adopted for DB: (a) use only over-land when (b) its internal quality assurance flag is highest and where (c) no high-quality DT retrieval exists. Further, once a pixel can potentially use a DB observation, it is used only after passing all of the equivalent DT quality assurance checks. Application of this approach yields a final MODIS assimilation-ready dataset that is quality assured to the same extent as that being used in the NAAPS but augmented by DB retrievals (intended to specifically help with dust and smoke over bright reflecting land areas).

The observational error for over-land and over-ocean MODIS AOD retrievals are also adapted directly from Zhang and Reid, 2006 (Table 4), Zhang et al., 2008 (eq. 5), and Hyer et al., 2011 (Table 3). These formulate the standard deviation of the MODIS error (the AOD RMSE) as a linear function of the retrieved MODIS AOD, where the level 2 10km retrievals are binned as needed and grouped into super-observations per 36km CMAQ grid-cell. Super-observations are defined as the mean MODIS-retrieved AOD among all quality assured level 2 10km retrievals per CMAQ 36km grid cell and located at the mean latitude/longitude of all valid retrievals within

that grid cell at the time of Terra or Aqua overpass. Coefficients from Zhang and Reid, 2006 (Table 4, DT over ocean) and Hyer et al., 2011 (Table 3, DT over land) are used to estimate the instrument error variance, whereas spatial data variation is estimated by the spatial sample variance from the averaging of MODIS ***Tau*** within each 36km grid cell. Within any one 36km grid cell, each super-observation thus also represents a temporal average ("oversample") of the acceptable satellite observations therein, consistent with how Zhu et al., 2014; Wilkins and deFoy, 2012, and other authors have utilized Ozone Monitoring Instrument (OMI) data.

The MODIS pre-processing software outputs the super-observation mean MODIS AOD at 550nm, the number of underlying accepted retrievals per super-observation, the standard deviation of the expected super-observation error as determined via the above-noted tables, the spatial variance of each super-observation, and the average latitude/longitude of all 10km retrievals comprising each super-observation. While we did not use the newer Collection 5 Dark Target error statistics for the development and testing reported here, we plan to update the error for Collection 5 Dark Target over-ocean retrievals from those published in Zhang and Reid, 2006 to the newer results following Shi et al., 2011 for the operational model that will be described in Part 2 of this paper.

The software also outputs an estimate of the (dominant) type of the observed MODIS aerosol as determined by a decision tree based on one or more of the aerosol type flags, retrieved AOD, Optical Depth Ratio Small ("Eta-MODIS water) and the Angstrom exponent. The decision trees for DB (land) and DT (land and water) are shown in Table 1, and they result in eight possible categorizations of the "likely" aerosol mix. This information is used later in preferentially

"nudging" model species during the step that inverts the final analyzed AOD to recover the aerosol species mixing ratios in the vertical (eq. 3). Levy, et al., 2010 elucidate significant limitations on the physical validity of the MODIS Collection 5 aerosol size parameters for DT over-land. More discussion on our approach – and its limitations, is provided below.

Table 1a here.

Table 1b here.

Table 1c here.

An estimate must also be made for the CMAQ AOD "background error." This is done following Zhang et al., 2008, adapted for CMAQ. In this method, CMAQ 2002 AOD estimates (computed using the revised RM approach without NO_2 extinction) are bi-linearly (and temporally, if needed) interpolated to each available AERONET latitude/longitude location within the CMAQ modeling domain. They are then paired with the AERONET observations. Model-observation pairs are subsequently binned in 0.1 ***Tau*** (i.e. AOD) intervals, and from these sets of binned pairs, the standard deviations of CMAQ errors are computed as a function of CMAQ estimated ***Tau***. For the full 2002 year including all AERONET locations CONUS-wide, the following baseline (non-assimilated) results were obtained:

$$\text{CMAQ\_}\boldsymbol{Tau}\text{\_error}_{\text{standard\_deviation}} \approx 0.13481 + 0.320207 * \boldsymbol{Tau}_{\text{CMAQ}} \qquad (12a)$$

Because the error model for MODIS AOD over-land is sub-divided into east and west land-areas of the CONUS (Hyer et al., 2011), a similar sub-division at -100 degrees west longitude was also

made for baseline CMAQ ***Tau*** errors. The following equations for eastern and western sections of the CONUS emerged from the 2002 data:

$$\text{CMAQ\_east\_}\boldsymbol{Tau}\text{\_error}_{\text{standard\_deviation}} \approx 0.220210 + 0.056791 * \boldsymbol{Tau}_{\text{CMAQ\_east}} \quad (12b)$$

$$\text{CMAQ\_west\_}\boldsymbol{Tau}\text{\_error}_{\text{standard\_deviation}} \approx 0.123674 + 0.419799 * \boldsymbol{Tau}_{\text{CMAQ\_west}} \quad (12c)$$

For the baseline model, the standard deviation of the errors rises only very slowly in the east as $\boldsymbol{Tau}_{\text{CMAQ\_east}}$ increases, indicative of CMAQ's "reasonably good," although low-biased, performance east of the Rockies (at least as measured for total AOD vis-à-vis the AERONET sites). The west tells a somewhat different story, with errors rising quite rapidly as $\boldsymbol{Tau}_{\text{CMAQ\_west}}$ increases there. As in Zhang et al., 2008, both MODIS and CMAQ make use of the independent AERONET surface AOD observations as a "ground-truth" means to quantify the relative importance of MODIS errors vis-à-vis CMAQ errors in the solution of equation (2). This approach contrasts with, for example, Liu et al., 2011 who use background error covariance matrices for each aerosol species in the GOCART model computed using the "NMC method" (Parrish and Derber, 1992).

The Q/A'd and processed MODIS DT/DB observations and their associated error estimates along with the above error model for CMAQ AOD provide the inputs needed to solve equation (2). This holds any time both observations and model estimates are available. In practice, MODIS granule overpasses are assigned to the nearest half-hour. CMAQ output is obtained on the half-hour and from it a background AOD estimate is calculated. The solver then minimizes a quadratic cost function resulting from equation (2), producing a final AOD analysis that – if the

statistics of the errors are exact – has the lowest possible overall error among all possible analyses that could result from the data available. CMAQ then continues its run until another set of MODIS observations becomes available, when the model is stopped again and a further assimilation is performed. Figure 2 shows an example of MODIS data valid between 1815 GMT and 1845 GMT overlaid as diamonds against the 36km CONUS grid depicting a daily composite of all valid MODIS retrievals "super-obbed" into their respective 36km CMAQ grid cells for an operational run made on July 16, 2015.

Figure 2 here

While the error covariance matrix for the MODIS observations is assumed diagonal, it is the correlation of the CMAQ errors (in space) that modulate the extent of the influence of any one set of observations within the final analysis. Again following Zhang et al., 2008 a typical second order auto-regressive function of the form found in equation (7) of that paper is employed:

$\mathbf{C}_{b(m,n)} = (1 + R_{mn}/L)\exp(-R_{mn}/L)$ (13), where

$\mathbf{C}_{b(m,n)}$ is the error correlation between two CMAQ grid cells, R_{mn} is the great circle distance between the two grid cells, and L is the horizontal error correlation length scale. L becomes, in some sense, a tuning parameter: the smaller the overall error correlation length, the "tighter" the region of influence of the observations on the final analysis. After testing, results described in Zhang et al., 2008, setting L = 2DX = 72km were used for the 2002 VISTAS initial implementation, but have since been reduced to L=54km for operational application.

Inverse Operator

The variational formulation in equation (2) makes it attractive to include possibly non-linear forward models in the solution approach. In this case, the **H** operator would become a Jacobean matrix **δ**(Aerosol-Concentration)/**δ**(Tau), potentially requiring either a tangent linear approximation to the revised IMPROVE equations or an outer loop (e.g. Daley and Barker, 2001, equations 5.2 and 6.2; Liu et al., 2011, equation 4). Following Zhang et al., 2008 the somewhat simpler inverse operator, whereby equation (2) is fully solved for the ***Tau*** increment and then equation (3) is used to independently recover the species concentration increments was chosen. The procedure iterates through the revised RM equations, calculating a revised ***Tau*** in the presence of equilibrated semi-volatile organics (SVOCs). The SVOC equilibration is accomplished in an inner iteration loop using the ORGAER3 sub-routine extracted from CMAQ. Within each iteration, preferential nudging of species increments is applied by utilizing the results of the appropriate decision tree until the equilibrated vertical profile of aerosol concentrations (in ug/m^3) converges to the updated optimal ***Tau***. The method accounts for the piece-wise linearity of **H** through iterative convergence, and is applied throughout the depth of the modeled atmosphere.

CASE-STUDY APPLICATION

To examine the impact of assimilating MODIS observations on the 2002 VISTAS CMAQ performance, a subset of 9 five-day cases that each feature elevated particulates/degraded visibility was selected. To comprise the set, events were chosen based on a range of processes responsible for visibility reduction. Selecting such a subset was required on two accounts – first, data from MODIS/Aqua was not available at all for the 2002 calendar year, while data from

MODIS/Terra (Collection 5.1) was only available at certain times. Second, limited computational resources made the ability to conduct an entire year of data-assimilating runs impractical. Nonetheless, the "full-year" error models (as described above) for both MODIS observations and CMAQ baseline run were applied within the case studies to better characterize the overall error climatologies; the developed error models are then used as a basis to provide "event-specific" error covariance matrices for each of the cases. Event-specificity arises because the previously described regression equations recover the error standard deviations for any given modeled grid cell unique to any retrieval time as a function of MODIS observed or CMAQ estimated AODs in that grid cell. However, no flow dependent errors are to be implied. Again, this approach is based on that implemented within the operational NAAPS.

Table 2 shows the original nine cases and their features. Unfortunately, the March 24th case had to be dropped due to lack of MODIS/Terra observations, leaving a total of eight five day cases for the assimilation verification/benchmark. The initial case selection could have benefitted from choosing a clean case to provide a cross-check that the assimilation was not spuriously creating AOD, however this has now been done as part of the operational implementation and will be discussed in Part 2 of the manuscript.

Table 2 here

Once the cases had been selected, daily composite MODIS AOD images were examined to gain a qualitative sense for the coverage (and thus the potential impact) that could be expected from assimilation. Clearly, significant cloud cover or snow reduces and/or even masks satellites' ability to contribute to AOD/pollutant assessment—and assimilation of the data into a model.

This is likely to be worse in northern hemisphere winter time, when cloud and snow cover are at a maximum. For example, little if any MODIS coverage of the Upper Midwest February nitrate event occurred due to cloudiness. To evaluate the cases, tile plots, scatter plots and statistics were developed for both baseline runs and benchmark assimilated runs (CMAQ-DA herein), for both total column AOD and for surface aerosol measurements collected at monitoring networks during the case periods. Statistics include the best fit line, RMSE, bias error, R^2, Index-of-Agreement (IA), and correlation-coefficient. These are all defined in the conventional way. While these were generated for each case independently, results aggregated across the eight cases will be presented here. The lack of ideal MODIS/Terra coverage of some of the events along with the complete lack of any MODIS/Aqua observations should be borne in mind throughout the discussion to follow.

Figure 3 here

Figure 3 shows CMAQ baseline versus CMAQ-DA results for total column aerosol optical depth. The figure reveals a striking improvement in the shape of the scatter about the 1:1 line, with the slope of the best fit line improving from 0.3242 to 0.5131, indicative of the reduction in low AOD bias due to the MODIS/Terra ***Tau*** assimilation. Table 3 shows the associated discreet statistical improvements: while the baseline model was biased nearly 50% low, the low bias in the assimilated model was reduced to ~20%. ***Tau*** mean absolute error (MAE) was reduced from 0.114 to 0.092, the RMSE improved from 0.1864 to 0.1532, R^2 improved from 0.401 to 0.468, and the Index of Agreement (IA) improved from 0.6511 to 0.7922. These improvements were

realized even though not all AERONET locations paired with CMAQ output experience a concurrent MODIS/Terra overpass.

As previously described, both MODIS and CMAQ error models (equations 12b and 12c) were independently developed for eastern and western US sub-domains and were applied as such for each of the case studies. Both CMAQ and MODIS had poorer error statistics in the western part of the US. Hyer et al., 2011 note that the western CONUS presents one of the greatest challenges for MODIS (DT) retrievals due to large errors. Plots (not shown) of baseline CMAQ versus AERONET observations also showed much larger scatter in the west. Previously it was noted that while Deep Blue retrievals were included in our assimilation--and were expected to benefit the west more than in the east--the DB error model is "borrowed" from the Dark Target over-land results (Hyer et al, 2011). Thus, in the first version of the system, *too much error could* be attributed to DB. This would result in not allowing it to provide as much correction to CMAQ as it potentially could.

Three surface measurement networks were used to evaluate the impact of AOD data assimilation on ground-level model aerosol species concentrations. The data from these networks was supplied by VISTAS and represents a subset of the same data used in the final VISTAS MPE (Morris et al. 2009). These data include observations from the EPA Federal Reference Method $PM_{2.5}$ and PM_{10} mass Network (FRM), the IMPROVE network, and the EPA Speciated Trends Network of $PM_{2.5}$ species (STN), now referred to as the Chemical Speciation Network. BAMS' rerun of the annual 2002 baseline showed negligible differences across all species at the surface as compared to the native VISTAS CMAQ 36km outputs. Thus, although in some cases the

metrics or presentation methods differ, our baseline results faithfully represent the performance obtained by the VISTAS MPE, with two caveats. First, because the VISTAS MPE was conducted east of the Rockies, observations used for species-specific evaluation were available only in the eastern half of the CONUS. Secondly, we used the VISTAS CMAQ 36km CONUS results as our baseline, whereas the VISTAS evaluation focused on their nested (within the 36km CONUS grid) eastern 12km grid. With this understanding, the potential for surface aerosol species improvements can be initially quantified.

The following mappings between CMAQ aerosol output and components measured by the three networks were followed. These are consistent with VISTAS and shown in Table 4. Again, results are aggregated over all eight 5-day cases.

Table 4 here

Twenty-four hour averaged total $PM_{2.5}$ mass in ug/m^3 was evaluated for FRM, IMPROVE, and STN networks by pairing CMAQ output with the observations at each station time and location throughout the averaging day. Figure 4 reveals that for the FRM network, which had the vast majority of valid $PM_{2.5}$ measurements, there is improvement in both slope (.547 versus .493) and intercept (5.548 versus 6.074) of the best-fit line (a versus b; top left versus top right). Similar improvement is seen in Figure 4 for the IMPROVE sites (c versus d; bottom left versus bottom right).

Figure 4 here

Table 5 presents $PM_{2.5}$ discreet statistical results for the networks, revealing consistent improvements in bias error, RMSE, R^2, and Index of Agreement across the networks. Within the FRM network, more than 10,000 data pairs from the aggregated set of 40 case days contributed. The overall bias in 24-hour average $PM_{2.5}$ mass decreases from an under-prediction of about -3.5 *ug*/m^3 to about -3 *ug*/m^3, whereas the RMSE decreases from ~9.3 *ug*/m^3 to approximately ~8.8 *ug*/m^3. Both the R^2 and IA statistics show improved skill as well. Clearly, assimilation of MODIS/Terra AOD has a positive impact on model skill in the eastern US for total surface $PM_{2.5}$.

Table 5 here

Organic carbon results, also representing 24-hour averages, were also encouraging. Scatter plots (not shown) from the IMPROVE and STN networks showed improvements in slope (both networks) and intercept (IMPROVE) of the best-fit lines (IMPROVE slope/intercept: 0.351-to-0.530 / 2.472-to-2.404; STN slope/intercept 0.348-to-0.448 / 2.459-to-2.560), with the improvement in slope for STN being more relevant than the marginal worsening of the intercept. This is supported by the across the board improvements in RMSE, R^2, and IA for both networks shown in Table 6.

Table 6 here

For elemental carbon (EC) measured by the STN network, the slope of the best-fit-line improves from 0.713 to 0.815 with little change in intercept (not shown), while for the IMPROVE network, the slope improves from 0.759 to 1.136, again with little change in intercept (not

shown). The discrete statistics shown in Table 7 indicate modest performance gains among the IMPROVE measurement sites (e.g. R^2 improves from 0.409 to 0.530) but very slight degradation at the STN sites. It appears that some STN network outliers (in which the baseline CMAQ was already too high) were nudged upwards by the assimilation resulting in the minor deterioration in EC statistics for that network (Table 7).

Table 7 here

The IMPROVE network offered the only set of viable measurements for fine soil dust and coarse material, again analyzed as 24-hour average concentrations. Scatter plots (not shown) revealed little change in either intercept or slope for either of these two constituents. Tables 8 and 9 hint at slight performance degradations for fine soil dust and enhancements for coarse matter, but the sample size is quite small. Moreover, the selected episode types (Table 2) suggest that these two constituents would not have been a significant fraction of the assimilated ***Tau*** signal.

Table 8 here

Table 9 here

DISCUSSION

Species Specific Nudging Algorithm

Levy et al., 2010 report significant limitations with Collection 5 based retrieved aerosol *properties* over land, such that the species-specific nudging algorithm that we implement may

not be globally justifiable for DT over land. Briefly, the MODIS algorithm look-up table (LUT) is based on three distinct fine mode models (sizes << 1.0*um*, including most smoke-related aerosol), and one coarse mode model generally assumed to be dust. The final AOD at .55*um* is in turn based on a weighting factor (ETA) between the coarse mode model and the most closely fit fine mode model. However, the determination of aerosol size properties by the algorithm is fully dependent on the assigned aerosol model type given the best fit to the LUT, thus the retrieved size properties are wholly dependent on the underlying assumptions contained within the four representative models. As Levy et al., 2010 conclude, in general MODIS size parameters are too burdened by a priori assumptions within the LUT for the errors in the retrieved size parameters to be globally quantifiable (against AERONET measured aerosol size properties, which are used as ground truth, see Figure 2 in that paper).

As shown in Table 1b, our algorithm for DT over-land is consistent with the information provided by the MODIS algorithm for Collection 5. For AOD < 0.2, we simply use the final assigned aerosol type without attempting any further discrimination. Noting that we never assimilate observations whose confidence flags are not the highest possible, a retrieved MODIS value of AOD=0.15 over land whose type flag indicates dust would contribute to preferential nudging of the CMAQ dust (coarse mode) species. However, within each 36km CMAQ grid cell there are usually >1 than one valid 10km retrieval (Levy et al., 2010). Again referring to Table 1b, if within that cell there was another valid retrieval with MODIS AOD = 0.30, we would first use its type information and then use its reported Angstrom Exponent (AE, see Levy et al., 2010 for a description of how the MODIS DT over-land AE is computed, along with its problems) to arrive at a final type categorization among the eight possible shown in Table 1. The additional

discrimination is theoretically consistent with Eck et al., 1999, who note that the AE is related to aerosol size whereby larger values of AE indicate smaller column-effective particles size, and conversely (Levy et al., 2010, pp. 10402). Thus, within each CMAQ grid cell occupied by one or more valid retrievals, we can compute the MODIS AOD retrieved fractions (MDFR) for each of the eight *categorical types*.

We then make use of this information in the inversion step (eq. 3) after the analyzed (cost-function-minimized) AOD is established by aggregating the retrieved *categorical fractions* to arrive at lumped AOD type fractions according to:

$$MDFR_{DUST} = MDFR_{cmdst} + MDFR_{ucdst} + 0.75 * MDFR_{cmdstfm} + 0.25 * MDFR_{fmsmkcm} \quad (14a)$$

$$MDFR_{SMOK} = MDFR_{fmsmk} + MDFR_{ucsmk} + 0.25 * MDFR_{cmdustfm} + 0.75 * MDFR_{fmsmkcm} \quad (14b)$$

$$MDFR_{MIXD} = MDF_{ucmixd} + MDFR_{sulf} \quad (14c),$$

where the sum of the final lumped AOD fractions "observed" by MODIS is guaranteed to = 1.0. But we still can't apply these lumped AOD fractions until they can be appropriated to the relevant CMAQ species. In the initial implementation, we consider the speciation provided to CMAQ by smoke and dust *emissions* respectively as shown in Tables 10 and 11. In practice this means that the final lumped $MDFR_{DUST}$ is apportioned (Table 10) to 70.2% ASOIL, 22% A25J, and 7.8% ACORS, where ASOIL is coarse (>2.5*um*) CMAQ dust (sand), A25J is a fine mode soil-dust species (<=2.5*um*), and ACORS is generalized coarse mode suspended aerosol. Table 11 shows the weightings applied to the lumped $MDFR_{SMOK}$ fraction based on the emissions of biomass burn material. All species are equally weighted for application to the lumped

$MDFR_{MIXD}$ fraction. Thus, any one species re-weighting is calculated using all of the lumped categorical fractions multiplied by the appropriate speciation weighting *per category* (Tables 10, 11, or no preference). As noted above, the inversion algorithm iterates using these initial weightings and the ratio of the background to analyzed AOD to arrive at a final model AOD that matches the variationally analyzed AOD. Care must be taken when the analyzed AOD represents a reduction of the background CMAQ AOD, so as not to allows species concentrations to become <=0.0*ug*/m3. We note that due to gravitational settling of airborne dust, the assimilated dust apportionment may not be completely faithful to the atmospheric dust apportionment.

Table 10 here.

Table 11 here.

While this approach is a reasonable first attempt, Levy et al., 2010 note that the derived AE cannot capture the variability in the ground truth – it is in general binary, indicating that either fine or coarse modes have been selected by the algorithm – that is, the ETA weighting over land is almost always either 0.0 or 1.0. They find that when MODIS indicates the dominance of one of the fine aerosol models, it typically agrees with AERONET; however MODIS tends to "find dust when there is none." However, they also note that for coarse dominated conditions of high AOD that are properly retrieved over land, MODIS typically underestimates by 20%, and that this underestimation is largest in heavy, dusty conditions. Given this, we would expect our algorithm to statistically over-nudge the CMAQ dust components slightly (especially at lower AOD values), and perhaps under nudge smoke or mixed aerosol components slightly across a very large land-based sample size of events, except for heavy dust events properly retrieved,

where due to the MODIS DT land low-bias our dust nudging could be underestimated. On the other hand, a large fraction of dust emitting events in the US come from the desert southwest, where Deep Blue is expected to be more accurate than DT. Hence at this juncture, our use of the combined DT/DB dataset plays to the strengths of DB and that may help mitigate some of the dust related problems with DT if the suspended plumes are localized to the dust emitting region. The relatively small sample size represented by our 40 case-days is almost certainly not large enough to have any statistically meaningful assessment of how our scheme is works versus quantifiable ground truth. Nonetheless, where DT retrievals are used over the continental US land-surface, the arrived at categorical AOD fractions are subject to the underlying assumptions (and weaknesses) of the MODIS DT-land retrieval algorithm as reported in Levy et al., 2010. In any event, the final model AOD always matches the analyzed AOD, even if the input speciated weighting factors cannot be fully trusted. A much larger sample size of CMAQ-DA results against speciated surface observations is needed to more fully assess our scheme.

Comparison of Results with Similar Studies and Implications for Operational Forecast Implementation

To help mitigate negative health consequences from exposure to fine particles, EPA estimates risk level using a five-color scale, based on the 24-hour average total $PM_{2.5}$ concentration as follows:

Table 12 here.

For this reason, the operational BAMS CMAQ-DA provides daily forecasts (out to five days) of 24-hour-average total surface $PM_{2.5}$ concentrations portrayed using the EPA color scale. Thus, any improvement in the model's ability to correctly forecast these color codes increases the confidence that official forecasters have in the model's guidance.

Evaluation of the effect of assimilating MODIS/Terra AOD data in the eastern half of the US for the 40 case-day 2002 development period shows that the overall low bias in CMAQ modeled total fine particle concentrations measured at the surface improves by 13.35%, considering an average weighted by the number of observations within each of the three networks (Table 5). Not surprisingly this is smaller than the 30% bias improvement than occurs in the ***Tau*** field (Table 3), simply because ***Tau***-based species increments must in general be applied throughout the depth of the CMAQ model atmosphere, not just at the surface. Similarly, the modeled total surface $PM_{2.5}$ RMSE improves by just over 6%, the R^2 statistic improves by 11.4%, and the Index-of-Agreement improves by 4.88%, again considering the weighted average across all measurement networks. As noted above, our results are valid for 24-hour model versus surface observation averages.

Organic species – a crucial component of $PM_{2.5}$ -- also improved significantly. Taking an ensemble average, sulfates, nitrates, and ammonium contribute almost 50% of total $PM_{2.5}$, with roughly 35% coming from organics. Elemental carbon (light absorbing) makes up 3-4%, with fine soil dust accounting for the other 10%. Known model difficulties representing both nitrates (especially in winter) and ammonium do exist, but the data-assimilation does affect these species as well. Since our analysis showed little if any improvement in fine soil dust and only a hint of

improvement in EC, $PM_{2.5}$ performance gains over the selected case days is mostly attributable to the other 85% of the CMAQ total $PM_{2.5}$ signal. We already noted that both the cases selected and the location of the speciated observations (eastern US) leads us to expect little impact from fine soil dust for this analysis.

For their single-day OI experiment, Tang et al., 2015 similarly report improvement in surface $PM_{2.5}$ bias. However, they also report what could be considerably worse results for $PM_{2.5}$ correlation coefficient – among all experiments, the statistically best run resulted in an R^2 value of 0.16 (r=0.40) across the CONUS, and R^2=0.048 (r=0.22) over the southeast US. They indicate (but do not explain the procedure) that hourly data pairs were used within the 24-hour experimental period, which could significantly affect their reported correlations due to sub-diurnal effects. Differences in the domain, experimental length, dates of application, assimilation algorithm, model resolution, and other nuances make conclusive quantitative comparison with our results nearly impossible.

For visibility applications, all of the modeled fine and coarse particle species contribute to surface visibility degradation per the revised IMPROVE equations. While complexity in coarse material composition arises near salt-water boundaries, well inland sea-salt should not be a factor. Taken alone, the negative bias in coarse matter improved slightly, by about 4%, with RMSE improvements around 2%. When considered against an "improved" R^2 of only 0.1828 versus a baseline of 0.1499 (Table 9), MODIS/Terra ***Tau*** assimilation provided only a small boost in the model's rather poor ability to capture overall coarse matter fate for the 40 case-days. Since the sample size was small, these increases are almost certainly statistically insignificant.

While DB retrievals are expected to help substantially with windblown (coarse) dust, as discussed this advantage should be largely limited to the desert southwest. In the east, the number of high quality Deep Blue retrievals that occur when Dark Target fails should be fairly small, if not negligible. More work is needed to further disentangle windblown dust issues, especially in light of the MODIS DT-land retrieval issues.

The most important metric for visibility applications is the aerosol optical depth. To derive the error model for CMAQ, a full year of baseline non-assimilated CMAQ results paired with "ground-truth" AERONET sun-photometer measurements was utilized. This was done for the full CONUS, as well as sub-dividing the domain into eastern and western sections. The latter two equations (12b and 12c above) were applied in the 2DVAR algorithm for each of the 8 five-day case periods. Because the assimilated model was not run for the full-year, it could not be used to re-estimate the full-year error equations in order to draw "before" versus "after" comparisons. Instead, we used the 40-day case study period to examine the improvement in the estimated error by re-estimating the error equations for both baseline and assimilated models, for both east and west sub-domains.

The results are shown in Table 13. In the east, there is unequivocal improvement in the modeled AOD errors, such that the overall standard deviation of the CMAQ AOD error as measured against surface sun photometer data remains nearly flat (slope of 0.00360) as concentrations increase. That is, *the errors grow much more slowly as a function of total modeled AOD in the assimilated versus baseline CMAQ models in the east*. Further, the assimilated model intercept is lower as well.

Table 13 here.

In the west, while there is improvement in the error range at smaller ***Tau*** (assimilated intercept of 0.04 versus baseline of 0.15), the error steadily grows larger due to the higher slope (0.50 versus 0.22), such that at ***Tau***=1.0, the standard deviation of the baseline model error is 0.3832, whereas for the assimilated model it is 0.5489. This is consistent with the previous discussion indicating that both the baseline CMAQ and MODIS DT retrievals have larger errors in the west.

Because of the uncertainty in the DB error model (now borrowed from DT), we cannot draw any definitive conclusions about how much, if any, improvement DB could ultimately make in the quality of the MODIS ***Tau*** retrievals in the west for data-assimilation, even though we think we could be overestimating the DB errors.

By way of comparison against our "progenitor approach," the NAAPS global model reported its baseline standard-deviation error equation as 0.20 + 0.4*$\boldsymbol{Tau}$ prior to implementing MODIS AOD data-assimilation, and 0.15 + 0.3*$\boldsymbol{Tau}$ after implementation (Zhang et al. 2008). For the 40-case days in the east, our baseline standard-deviation error equation is ~0.22 + 0.09*$\boldsymbol{Tau}$ prior to implementing MODIS AOD data-assimilation, and ~0.18 + 0.003*$\boldsymbol{Tau}$ after implementation. Our improvement compares favorably (perhaps better, considering the relative slope improvement) with the NAAPS error improvement. In the west our assimilated model improves for lower values of ***Tau*** but error standard-deviations rise more rapidly and exceed the baseline for values of ***Tau*** greater than about 0.50.

For operational application, one might consider nesting a more complete process model like CMAQ within a global lower resolution forecast model like NAAPS in which both assimilate AOD data using very similar algorithms. Equation (12) indicates the baseline (non-assimilated) CMAQ model full-domain full-year error model was 0.13481 + 0.320207*$\boldsymbol{Tau}$. Although model resolution and coverage differences prevent quantitative conclusions, it is interesting that this baseline error is actually slightly better than the final assimilated NAAPS global model error. This would support the idea that there could be significant value in nesting a more "complete process model" such as CMAQ inside a high-quality global model like NAAPS to obtain forecast aerosol boundary conditions for the nested CMAQ.

Other authors describe results that are qualitatively consistent with ours, but due to significant differences in experimental design, conclusive quantitative comparisons are again not possible. For example, using optimal interpolation and CMAQ over east-Asia and including improved emissions, Park et al., 2011 (Table 8 therein) showed that model simulated AOD correlations improved from about r=.67 (R^2=.45) to r=.76 (R^2=.59) when all four seasons' results from their 2006 simulation year were averaged. For the 40-case days we used in development, the ***Tau*** correlation coefficient improved from r=0.633 to r=0.684, while our assimilated ***Tau*** RMSE was lower than Park et al.'s. Liu et al., 2011 did not present statistical results. However, hourly time series plots over a simulation week at six AERONET locations in east-Asia indicate obvious improvement in low AOD bias for the assimilated WRF-CHEM model using GOCART.

AOD forecasts were also evaluated by Schwartz et al., 2012, who showed that over their six-week experimental period WRF-CHEM (GOCART) assimilation of both MODIS AOD and EPA

AIRNow (http://www.airnow.gov) surface $PM_{2.5}$ observations resulted in an improved in AOD correlation coefficient at AERONET sites from the "noDA" baseline of r=0.288 (R^2 =.083) to r=0.319 (R^2=.101). In their case the statistics were calculated using model vs. MODIS-***Tau*** (as opposed to AERONET) observations, making comparisons with other studies challenging. (Time series at several AERONET locations are given with AERONET observations plotted, but model-AERONET ***Tau*** improvement statistics are not provided). Improvements in bias, de-biased RMSE, and correlation coefficients for hourly forecast surface $PM_{2.5}$ are also presented in time-series (not tabular) form. Visual assessment indicates that combined surface $PM_{2.5}$ and MODIS ***Tau*** assimilation provides the most improvement and that correlation against EPA AIRNow surface $PM_{2.5}$ observations increases from r=~0.40 (R^2=0.16) to r=~0.55 (R^2=.30). Looking at Table 5, our surface $PM_{2.5}$ correlations improve from a baseline of ~r=.67 (R^2 = .46) to ~r=.72 (R^2=.52). Here again, their statistics are based on hourly data-pairs, whereas ours are based on 24-hour averaged data-pairs (since this is the metric used by EPA to set the health effects standard).

CONCLUSION

This paper has described the initial development and validation of a version of the CMAQ air quality model that assimilates MODIS aerosol optical depth measurements from both the Terra and Aqua polar orbiting satellites in real-time (Collection 5). Our approach is unique to versions of CMAQ that are being applied for operational forecasting in that we implement an observation-space variational algorithm for computing the final analyzed AOD fields. In contrast to simpler optimal interpolation, our approach allows for the utilization of more robust statistically

consistent weighting. Furthermore, in addition to DT retrievals, we make use of the newer DB retrievals to augment and improve the quality of the MODIS AOD data over brighter reflecting surfaces. While clearly subject to the uncertainties of the MODIS retrieval algorithms, our species-nudging approach based on the best available aerosol physical property data available within the MODIS retrievals is also innovative.

The initial offline development was conducted using a vetted annual case study for baseline year 2002 in partnership with the VISTAS Regional Planning Organization. The CMAQ run was first reproduced retrospectively and then modified to assimilate the ***Tau*** observations using 8 representative five-day events. Over these 40-case days in the eastern US, the overall low bias in modeled total fine particle concentration improved by 13.35%, considering a weighted average of bias improvements among all measurement networks. Similarly, the modeled total $PM_{2.5}$ RMSE improved by just over 6%, the R^2 statistic improved by 11.4%, and the Index-of-Agreement improved by 4.88%, again considering a weighted average across all measurement networks. With respect to total column aerosol optical depth, unequivocal improvement in total AOD east of the Rockies was demonstrated, such that the revised standard deviation of the AQF-DSS AOD error as measured against surface sun photometer data has a lower initial value (intercept) and remains nearly flat as concentrations increase. Further, the assimilated model intercept was lower as well. In the western U.S., the impact of MODIS AOD data-assimilation was less evident. However, a better error model for the new Deep Blue retrieval method, which holds promise over the brighter reflecting land-surfaces characteristic there, should help rectify this. Notwithstanding, MODIS coverage of dust-based events was very limited, restricting our

ability to fully assess its potential to increase forecast skill in the west as measured within the 2002 VISTAS baseline run.

Unfortunately, only MODIS/Terra observations were available for the initial VISTAS 2002 baseline development period. However, had MODIS/Aqua retrievals been available, the density of high quality assimilated observations would have approximately doubled, almost certainly resulting in larger statistical improvements than were realized with MODIS/Terra alone. Nevertheless, our results compare very favorably against a number of contemporary studies which assimilate MODIS ***Tau*** data into air quality simulation models, including CMAQ, and they serve as the basis for our decision to extend the retrospective CMAQ-DA to real-time/operational forecast mode. In Part 2 of the paper, we will describe the operational forecast implementation and real-time improvement of the BAMS CMAQ-DA model along with an assessment of forecast performance for both warm and cool seasons across the entire CONUS.

ACKNOWLEDGEMENTS

Work to develop and test the MODIS data-assimilation capability within CMAQ was supported by the NASA Applied Sciences Program under Cooperative Agreement NNA07CN15A. The authors would like to thank Dr. M.J. Jeong, Ms. Clair Salustro, and Mr. Jeremy Warner at NASA Goddard Space Flight Center, along with Dr. Rudolf Husar and Mr. Kari Hoijvari at Washington University in St. Louis for significant contributions to the development effort. The authors would also like to thank Mr. Don Olerud, Dr. Carlie Coats, and Mr. Robert Imhoff of Baron Advanced Meteorological Systems for many fruitful discussions, along with three anonymous reviewers who helped to improve the manuscript.

REFERENCES

Binkowski, F. S. and S. J. Roselle. 2003. Models-3 Community multiscale air quality (CMAQ) model aerosol component 1. Model description. *J. Geophys. Res.-Atm.* **10**8, 4183, doi:10.1029/2001JD001409, D6

Byun, D. W., and J. S. Ching. 1999. Science Algorithms of the EPA Models-3 Community Multiscale Air Quality (CMAQ) Modeling System. *U. S. Environmental Protection Agency* Rep. **EPA-600/R-99/030**, 727 pp. [Available from Office of Research and Development, EPA, Washington, DC 20460.]

Chin, M., P. Ginoux, S. Kinne, B. N. Holben, B. N. Duncan, R. V. Martin, J. A. Logan, A. Higurashi, and T. Nakajima. 2002. Tropospheric aerosol optical thickness from the GOCART model and comparisons with satellite and sunphotometer measurements. *J. Atmos. Sci.* **59**, 461-483. doi:10.1175/1520-0469(2002)059%3C0461:TAOTFT%3E2.0.CO;2

Cohn, S.E., A. da Silva, J. Guo, M. Sienkiewicz, and D. Lamich. 1998. Assessing the effects of data selection with the DAO Physical-Space Statistical Analysis System. *Mon. Wea. Rev.* **126**, 2913-2926. doi:10.1175/1520-0493(1998)126%3C2913:ATEODS%3E2.0.CO;2

Coats, C. J., and M. R. Houyoux. 1996. Fast Emissions Modeling with the Sparse Matrix Operator Kernel Emissions (SMOKE) Modeling System. *The Emissions Inventory: Key to Planning, Permits, Compliance, and Reporting.* **Air & Waste Management Association**, New Orleans, LA, 539-548.

Daley, R. and Barker, E. 2001. *NAVDAS Source Book*. **NRL/PU/7530-01-444**, Naval Research Laboratory, Monterey, CA, 163 pp.

Davidson, P., K. Schere, R. Draxler, S. Kondrangunta, R. A. Wayland, J. F. Meagher, and R. Mathur, 2008. Toward a US National Air Quality Forecast Capability: Current and Planned Capabilities. **Air Pollution Modeling and Its Application** *XIX*. C. Borrego and A.I. Miranda (Eds.), 226-234, ISBN978-1-4020-8452-2 Springer, The Netherlands.

Eck, T. F., B. N. Holben, J. S. Reid, O. Dubovik, A. Smirnov, N. T. O'Neill, I. Slutsker, and S. Kinne. 1999. Wavelength dependence of the optical depth of biomass burning, urban, and desert dust aerosols. *J. Geophys. Res-Atm.* **108**: doi:10.1029/1999JD900923

Eder, B., D. Kang, A. Stein, J. McHenry, G. Grell, and S. Peckham. 2005. Development of an evaluation protocol and performance benchmark as part of the New England Air Quality Forecasting pilot program. *J. Air Waste Manag. Assoc*. **55**, 20-27.

Grell, G. A., S. E. Peckham, R. Schmitz, S. A. McKeen, G. Frost, W. C. Skamarock and B. Eder. 2005. Fully coupled online chemistry within the WRF model. *Atmos. Environ.* **39**, 6957-6975. doi:10.1016/j.atmosenv.2005.04.027

Hsu, N.Christina, S.-C. Tsay, M. D. King, and J. R. Herman. 2004. Aerosol properties over bright-reflecting source regions. *IEEE Trans. on Geosci. and Remote Sensing* **42**(3), 557-569. doi:10.1109/TGRS.2004.824067

Hyer, E. J., J. S. Reid, and J. Zhang. 2011. An over-land aerosol optical depth data set for data assimilation by filtering, correction, and aggregation of MODIS Collection 5 optical depth retrievals. *Atmos. Meas. Techniques* **4**, 379-408. doi:10.5194/amt-4-379-2011

Interagency Monitoring of PROtected Visual Environments (IMPROVE). 2007. Revised IMPROVE Algorithm for Estimating Light Extinction from Particle Speciation Data. Available:

http://vista.cira.colostate.edu/improve/publications/graylit/019_RevisedIMPROVEeq/RevisedIMPROVEAlgorithm3.doc. (accessed July 20, 2015).

Jeong, M. J., and N.Christina Hsu. 2008. Retrievals of aerosol single-scattering albedo and effective aerosol layer height for biomass-burning smoke: Synergy derived from "A-Train" sensors. *Geo. Res. Lett.* **35**, L24801, doi:10.1029/2008GL036279

Kleist, D. T., D. F. Parrish, J. C. Derber, R. Treadon, W.-S. Wu, and S. Lord. 2009. Introduction of the GSI into the NCEP Global Data Assimilation System. *Wea. Forecasting* **24**, 1691–1705. doi:10.1175/2009WAF2222201.1

Lee, P., R. Saylor, H. C. Kim, D. Tong, Y. Kim, A. Stein, T. Chai, Y. Choi, Y. Tang, J. Huang, J. McQueen, M. Tsidulko, H. C. Huang, C. H. Lu, I. Stajner, K. Wedmark, and P. Davidson. 2012. Strong Influences of Land Use Land Cover Characterization on Air Quality Forecast Modeling. *14th Conf. on Atmospheric Chemistry*. **Amer. Meteor. Soc**., New Orleans, La., 2012.

Levy, R. C., L. Remer., S. Mattoo, E. Vermote, and Y.J. Kaufman. 2007. Second-generation operational algorithm: Retrieval of aerosol properties over land from inversion of Moderate Resolution Imaging Spectroradiometer spectral reflectance. *J. Geophys. Res-Atm.* **112,** D13211, doi:10.1029/2006JD007811

Levy, R. C., L.A. Remer, R. G. Kleidman, S. Mattoo, C. Ichoku, R. Kahn, and T.F. Eck. 2010. Global evaluation of the Collection 5 MODIS dark-target aerosol products over land. *Atmos. Chem. Phys.* **10**, 10399-10420. doi:10.5194/acp-10-10399-2010

Liu, Z., Q. Liu, H.-C. Lin, C. S. Schwartz, Y.-H. Lee, and T. Wang. 2011. Three-dimensional variational assimilation of MODIS aerosol optical depth: Implementation and application to a dust storm over East Asia. *J. Geophys. Res-Atm.* **116**, D23206. doi:10.1029/2011JD016159

Malm, W.C., J.F. Sisler, D. Huffman, R.A. Eldred and T.A. Cahill. 1994. Spatial and seasonal trends in particle concentration and optical extinction in the United States. *J. Geophys. Res-Atm.* **99**(D1), 1347-1370, doi:10.1029/93JD02916

Mathur, R., U. Shankar, A. Hanna, M.T. Odman, J.N.McHenry, C.J. Coats, Jr., K. Alapaty, A.Xiu, S. Arunachalam, D.T. Olerud, Jr., D.W. Byun, K.L. Schere, F.S. Binkowski, J.K.S. Ching, R.L. Dennis, T.E.Pierce, J.E. Pleim, S.J. Roselle, and Jeffrey O. Young. 2005. The Multiscale Air Quality Simulation Platform (MAQSIP): Initial applications and performance for tropospheric ozone and particulate matter. *J. Geophys. Res.-Atm.* **110**, D13308, doi:1029/2004JD004918

McHenry, J.N., F.S. Binkowski, J. S. Chang, and D. Hopkins. 1992. The tagged species engineering model. *Atmos. Environ.* **26**A, 8, 1427-1443. doi:10.1016/0960-1686(92)90128-8

McHenry, J.N., N. Seaman, C. Coats, A. Lario-Gibbs, J. Vukovich, N. Wheeler, and E. Hayes. 1999. Real-time nested mesoscale forecasts of lower tropospheric ozone using a highly optimized coupled model numerical prediction system. *Symposium on Interdisciplinary Issues in Atmospheric Chemistry.* **Amer. Meteor. Soc.**, Dallas, TX, 1999.

McHenry, J.N, N. Seaman, C. Coats, D. Stauffer, A. Lario-Gibbs, J. Vukovich, E. Hayes, and N. Wheeler. 2000. The NCSC-PSU numerical air quality prediction project: initial evaluation,

status, and prospects. *Proc. Symposium on Atmospheric Chemistry Issues in the 21st Century*, **Amer. Meteor. Soc.**, Long Beach, CA, 95-102, 2000.

McHenry, J.N., C. Coats, B. Cameron, J. Vukovich, A. Trayanov, and T. Smith. 2001. High-resolution real-time ozone forecasts for the August-September Texas AQS-2000 (Houston) field study: forecast process and preliminary evaluation. *Millennium Symposium on Atmospheric Chemistry*, **Amer. Meteor. Soc**., Albuquerque, NM, 186-193, 2001.

McHenry, J.N., W.F. Ryan, N.L. Seaman, C.J. Coats, J. Pudykeiwicz, S. Arunachalam, and J. Vukovich. 2004. A real-time Eulerian photochemical model forecast system: Overview and initial ozone forecast performance in the NE U.S. Corridor. *Bull. Am. Met. Soc.* **85**(4), 525-548. doi:10.1175/BAMS-85-4-525

McKeen, S., J. Wilczak, G. Grell, I. Djalalova, S. Peckham, E.-Y. Hsie, W. Gong, V. Bouchet, S. Menard, R. Moffet, J. McHenry, J. McQueen, Y. Tang, G.R. Carmichael, M. Pagowski, A. Chan, and T. Dye. 2005. Assessment of an ensemble of seven real-time ozone forecasts over Eastern North America during the summer of 2004. *J. Geophys. Res.-Atm.* 110, D21307, doi:10.1029/2005JD005858

McKeen, S., S. H. Chung, J. Wilczak, G. Grell, I. Djalalova, S. Peckham, W. Gong,V. Bouchet, R. Moffet, Y. Tang, G. R. Carmichael, R. Mathur, and S. Yu. 2007. Evaluation of several PM forecast models using data collected during the ICARTT/NEAQS 2004 field study. *J. Geophys. Res.-Atm.* **112**, D10S20, doi:10.1029/2006JD007608

Morris, R.E., B.Koo, A. Guenther, G. Yarwood, D. McNally, T.W. Tesche, G. Tonneson, J. Boylan, and P. Brewer. 2006. Model sensitivity evaluation for organic carbon using two multi-

pollutant air quality models that simulate regional haze in the southeastern United States. *Atmos. Env.* **40**(2006) 4960-4972. doi:10.1016/j.atmosenv.2005.09.088

Morris, R.E., B. Koo, P. Piyachaturawat, G. Stella, D. McNally, C. Loomis, C.-J. Chien, G. Tonnesen. 2009. *Technical Support Document for VISTAS Emissions and Air Quality Modeling to Support Regional Haze State Implementation Plans*. **ENVIRON Intl. Corp**, 773 San Marin Drive, Suite 2115, Novato, CA 94998, 253pp.

Pagowski, M., and G. Grell. 2012. Experiments with the assimilation of fine aerosols using an ensemble Kalman filter. *J. Geophys. Res.-Atm.* **117**, D21302, doi:10.1029/2012JD018333

Pagowski, M., Z. Liu, G. Grell, M. Hu, H.-C. Lin, and C. S. Schwartz. 2014. Implementation of aerosol assimilation in Gridpoint Statistical Interpolation (v. 3.2) and WRF-Chem (v. 3.4.1). *Geosci. Model Dev.*, **7**, 1621-1627. doi:10.5194/gmd-7-1621-2014

Pan, L., D. Tong, P. Lee, H.-C. Kim, and T. Chai. 2012. Assessment of NO_x and O_3 forecasting performances in the U.S. National Air Quality Forecasting Capability before and after the 2012 major emissions updates. *Atmos. Environ.*, **95**, 610-619. doi:10.1016/j.atmosenv.2014.06.020

Park, R.S., C.H. Song, K. M. Han, M. E. Park, S.-S. Lee, S.-B. Kim, and A. Shimizu. 2011. A study on the aerosol optical properties over East Asia using a combination of CMAQ-simulated aerosol optical properties and remote-sensing data via a data assimilation technique. *Atmos. Chem. Phys.*, 11, 12275–12296. doi:10.5194/acp-11-12275-2011

Pitchford, M., W. Malm, B. Schichtel, N. Kumar, D. Lowenthal, and J. Hand. 2007. Revised algorithm for estimating light extinction from IMPROVE particle speciation data. *J. Air Waste Manag. Assoc.* **57**(11): 1326-36.

Roy, B., R. Mathur, A. Gilliland, and S. Howard. 2007. A comparison of CMAQ-based aerosol properties with IMPROVE, MODIS, and AERONET data. *J. Geophys. Res.-Atm.* **112**, D14301, doi:10.1029/2006JD008085

Schwartz, C.S., Z. Liu, H-C Lin, and S. McKeen. 2012. Simultaneous three-dimensional variational assimilation of surface fine particulate matter and MODIS aerosol optical depth. *J. Geophys. Res.-Atm.* **117**, D13202, doi:10.1029/2011JD017383

Shi, Y., J. Zhang, J.S. Reid, B. Holben, E.J. Hyer, and C. Curtis. 2011. An analysis of the Collection 5 MODIS over-ocean aerosol optical depth product for its implication in aerosol assimilation. *Atmos. Chem. Phys.* **11**, 557-565. doi:10.5194/acp-11-557-2011

Skamarock, W. C., and J. B. Klemp. 2008. A time-split nonhydrostatic atmospheric model for research and NWP applications. *J. Comp. Phys.* **227**, 7, 3465-3485, doi:10.1016/j.jcp.2007.01.037

Stajner, I., P. Lee, J. T. McQueen, R. Draxler, G. Manikin, K. Wedmark, and T. McClung. 2012. Expansion of NOAA's National Air Quality Forecast Guidance. *Proc. 14th Conf. on Atmospheric Chemistry*. **Amer. Meteor. Soc.**, New Orleans, La., 2012.

Sousan, S., J. Baek, N. Kumar, J. Oleson, S. Spak, G. Carmichael, and C. Stanier. 2010. Use of Surface Measurements and MODIS Aerosol Optical Depth for Improved Model Based $PM_{2.5}$

Prediction in the United States. *2010 Conference of the Community Modeling and Analysis Center*, available: https://www.cmascenter.org/conference/2010/agenda.cfm, 2010.

Parrish, D.F. and J.C. Derber, 1992. The National Meteorological Center's Spectral Statistical Interpolation Analysis System. *Mon. Weather Rev.* **120**, 8, 1747–1763. doi:10.1175/1520-0493(1992)120%3C1747:TNMCSS%3E2.0.CO;2

Wilkins, J.L., and B. de Foy, 2012, Oversampling OMI SO2 to characterize large point sources, pollution transport and SO2 lifetimes in the atmosphere. **American Geophysical Union**, Fall Meeting 2012, abstract #A21B-0055. Accessed September 11, 2015; http://adsabs.harvard.edu/abs/2012AGUFM.A21B0055W

Wu, W.-S., D.F. Parrish, and R.J. Purser. 2002. Three-dimensional variational analysis with spatially inhomogeneous covariances. *Mon. Weather Rev.* **130**, 2905–2916. doi:10.1175/1520-0493(2002)130<2905 TDVAWS>2.0.CO;2

Zhang, J., J.S. Reid, D.L Westphal, N.L. Baker, and E.J. Hyer. 2008. A system for operational aerosol optical depth data assimilation over global oceans. *J. Geophys. Res.*-Atm. **113**, D10208, doi:10.1029/2007JD009065

Zhang, J., and J.S. Reid. 2006. MODIS aerosol product analysis for data assimilation: assessment of over-ocean level 2 aerosol optical thickness retrievals. *J. Geophys. Res.-Atm*. **111**, D22207, doi:10.1029/2005JD006898

Zhang, Y., M. Bocquet, V. Mallet, C. Seigneur, and A. Baklanov. 2012a. Real-time air quality forecasting, part I: History, techniques, and current status. *Atmos. Environ.,* **60**, 632–655. doi:10.1016/j.atmosenv.2012.06.031

Zhang, Y., M. Bocquet, V. Mallet, C. Seigneur, and A. Baklanov. 2012b. Real-time air quality forecasting, part II: State of the science, current research needs, and future prospects. *Atmos. Environ.*, **60**, 656–676. doi:10.1016/j.atmosenv.2012.02.041

Zhu, L., D. Jacob, L. Mickley, E. Marais, D. Cohan, Y. Yoshida, B. Duncan, G. Abad, and K. Chance, 2014. Anthropogenic emissions of highly reactive volatile organic compounds in eastern Texas inferred from oversampling of satellite (OMI) measurements of HCHO columns. *Env. Res. Letters*, **9**, 11, doi:10.1088/1748-9326/9/11/114004

Table 1a: MODIS-retrieved Aerosol Type Decision Tree: Dark-Target Over Ocean

MODIS AOT	**Optical Depth Ratio Small Ocean**	**Angstrom Exponent**	**Mixed Aerosol Unclassified** (ucmixd)	**Coarse Mode Dust plus some Fine Material** (cmdstfm)	**Coarse Mode Dust** (cmdst)	**Dust Unclassified** (ucdst)	**Fine Mode Smoke plus some Coarse Material** (fmsmkcm)	**Fine Mode Smoke** (fmsmk)	**Smoke Unclassified** (ucsmk)	**Sulfate** (sulf)
< 0.2	**Ignored**	**Ignored**	**X**							
>= 0.2	**< 0.6 (Dom. Coarse**	**<0.1**			**X**					
		0.1 <= AE < 0.7		**X**						

	Mode)	**>= 0.7**				**X**				
	>= 0.6 (Dom. Fine Mode)	**> 1.2**						**X**		
		0.7 < AE <= 1.2					**X**			
		<= 0.7							**X**	

Table 1b: MODIS-retrieved Aerosol Type Decision Tree: Dark-Target Over Land

MODIS AOT	**Aerosol Type Flag (Land)**	**Angstrom Exponent**	**Mixed Aerosol Unclassified** (ucmixd)	**Coarse Mode Dust plus some Fine Material** (cmdstfm)	**Coarse Mode Dust** (cmdst)	**Dust Unclassified** (ucdst)	**Fine Mode Smoke plus some Coarse Material** (fmsmkcm)	**Fine Mode Smoke** (fmsmk)	**Smoke Unclassified** (ucsmk)	**Sulfate** (sulf)
< 0.2	**Mixed**	**Ignored**	**X**							
	Dust	**Ignored**				**X**				
	Smoke or Heavy Absorbing Smoke	**Ignored**							**X**	

	Sulfate	**Ignored**								**X**
>= 0.2	**Mixed**	**Ignored**	**X**							
	Dust	**<0.1**			**X**					
		0.1 <= AE < 0.7		**X**						
		>= 0.7				**X**				
	Smoke or Heavy Absorbing Smoke	**> 1.2**						**X**		
		0.7 < AE <= 1.2					**X**			
		<= 0.7							**X**	
	Sulfate	**Ignored**								**X**

Table 1c: MODIS-retrieved Aerosol Type Decision Tree: Deep Blue Over Land

MODIS AOT	**Aerosol Type Flag (Land)**	**Angstrom Exponent**	**Mixed Aerosol Unclassified** (ucmixd)	**Coarse Mode Dust plus some Fine Material** (cmdstfm)	**Coarse Mode Dust** (cmdst)	**Dust Unclassified** (ucdst)	**Fine Mode Smoke plus some Coarse Material** (fmsmkcm)	**Fine Mode Smoke** (fmsmk)	**Smoke Unclassified** (ucsmk)	**Sulfate** (sulf)
< 0.2	**Mixed**	**Ignored**	**X**							
	Dust	**Ignored**				**X**				
	Smoke	**Ignored**							**X**	
	Sulfate	**Ignored**	**X**							
	Mixe	**Ignore**	**X**							

>= 0.2	**d**	**d**								
	Dust	**<0.1**			**X**					
		0.1 <= AE < 0.7		**X**						
		>= 0.7				**X**				
	Smoke	**> 1.2**						**X**		
		0.7 < AE <= 1.2					**X**			
		<= 0.7							**X**	
	Sulfate	**Ignored**	**X**							

Table 2: Eight five-day benchmark cases featuring a visibility reducing event from 2002.

Five Day Case Ending (2002)	Feature
February 7	Upper Midwest Nitrate Aerosol
March 24	Texas Dust*
July 1	Eastern US Stagnation Pollution
July 7	Quebec Fire, SE US Biogenic Organic
July 19	Eastern US Mixed Aerosol
July 30	Texas Sahara Dust
August 3	Oregon Smoke and Eastern US Sulfate
August 12	Eastern US fine-particulate and ozone
September 8	Midwest fine-particulate and ozone

*MODIS observations unavailable

Table 3. Improvement in CMAQ ***Tau*** Estimation Using MODIS AOD Data Assimilation as compared to Baseline CMAQ for 40 "case days" within the VISTAS 2002 annual simulation.

40 Case Days Statistics	**#PAIRS**	**MODIS *Tau* Average**	**CMAQ *Tau* Average**	**Bias Error**	**MAE**	**RMSE**	**R^2**	**Index of Agreement**
CMAQ baseline	19488	0.2127	0.1132	-0.0995	0.1147	0.1864	0.4012	0.6511
CMAQ with MODIS *Tau* Assimilation	19488	0.2127	0.1718	-0.0408	0.0924	0.1532	0.4681	0.7922

Table 4: CMAQ aerosol species mappings to surface measured aerosol components at three networks used in data-assimilation verification.

Evaluated Component and Network	CMAQ V4.51_(soamods) Species
Total $PM_{2.5}$ (IMPROVE, FRM, STN)	ASO4I + ASO4J + ANO3I + ANO3J + AORGAI + AORGAJ + AORGPAI + AORGPAJ + AORGBI + AORGBJ + ASOC1J + ASOC1I + ASOC2I + ASOC2J + ASOC3I + ASOC3J + AECI + AECJ + A25I + A25J + ANH4I + ANH4J
Organic Carbon (IMPROVE, STN)	AORGAI + AORGAJ +

	AORGPAI + AORGPAJ + AORGBI + AORGBJ + ASOC1J + ASOC1I + ASOC2I + ASOC2J + ASOC3I + ASOC3J
Light Absorbing Carbon (STN, IMPROVE)	AECI + AECJ
Fine Soil Dust (IMPROVE)	A25I + A25J
Coarse Matter (IMPROVE)	ACORS + ASOIL + ASO4K + ACLK + ANAK

Table 5: CMAQ total $PM_{2.5}$ results for baseline versus assimilated case-days from various measurement network sites for VISTAS baseline evaluation year 2002.

Network	**Run-Type**	**Number of Pairs**	**Bias (*ug*/m3)**	**RMSE (*ug*/m3)**	**R^2**	**Index of Agreement**
FRM	Baseline	10197	-3.5147	9.3265	0.4752	0.7760
	Assimilated	10197	-3.0307	8.7903	0.5218	0.8100
IMPROVE	Baseline	445	-3.0932	8.3193	0.4385	0.7551
	Assimilated	445	-2.7701	7.5179	0.5395	0.8114
STN	Baseline	1108	-5.5152	13.6227	0.3726	0.6768
	Assimilated	1108	-4.9363	12.6576	0.4526	0.7343

Table 6. CMAQ total Organic Carbon results for baseline versus assimilated case-days from various measurement network sites for VISTAS baseline evaluation year 2002.

Network	**Run-Type**	**Number of Pairs**	**Bias (*ug*/m3)**	**RMSE (*ug*/m3)**	**R^2**	**Index of Agreement**
IMPROVE	Baseline	446	0.1208	4.1806	0.3593	0.6946
	Assimilated	446	0.7033	3.5302	0.5626	0.8267
STN	Baseline	1106	-1.8812	5.9147	0.4246	0.6896
	Assimilated	1106	-1.1139	5.2519	0.5151	0.7806

Table 7. CMAQ total Elemental Carbon results for baseline versus assimilated case-days from various measurement network sites for VISTAS baseline evaluation year 2002.

Network	**Run-Type**	**Number of Pairs**	**Bias (*ug*/m3)**	**RMSE (*ug*/m3)**	**R^2**	**Index of Agreement**
IMPROVE	Baseline	446	-0.0712	0.3686	0.4095	0.7848
	Assimilated	446	0.0681	0.4195	0.5297	0.8006
STN	Baseline	1106	0.1031	0.6896	0.2051	0.6030
	Assimilated	1106	0.2827	0.8398	0.1956	0.5440

Table 8. CMAQ total Fine Soil Dust for baseline versus assimilated case-days from various measurement network sites for VISTAS baseline evaluation year 2002.

Network	**Run-Type**	**Number of Pairs**	**Bias (*ug*/m3)**	**RMSE (*ug*/m3)**	**R^2**	**Index of Agreement**
IMPROVE	Baseline	443	-0.1573	2.7206	0.0220	0.3063
	Assimilated	443	-0.0160	2.7616	0.0137	0.2883

Table 9. CMAQ total Coarse Matter for baseline versus assimilated case-days from various measurement network sites for VISTAS baseline evaluation year 2002.

Network	**Run-Type**	**Number of Pairs**	**Bias (*ug*/m3)**	**RMSE (*ug*/m3)**	**R^2**	**Index of Agreement**
IMPROVE	Baseline	429	-4.5660	7.6191	0.1499	0.4017
	Assimilated	429	-4.3807	7.4448	0.1828	0.4070

Table 10: Allocation of dust emissions flux to CMAQ species by percent.

Windblown Dust: Percentage of Emitted Flux	**CMAQ Species Allocation**	**Species Size**
70.2%	ASOIL	Coarse
22%	A25J	Fine
7.8%	ACORS	Coarse

Table 11: Allocation of biomass burn emissions flux to CMAQ species by percent.

Biomass Burn Smoke: Percentage of Emitted Flux	**Species Allocation**	**Species Size**
1%	ACORS	Course
9%	ASOIL	Course
69.3%	ORGPAI + ORGPAJ	Fine
14.4%	ECI + ECJ	Fine
4.32%	A25J	Fine
1.8%	SO4I + SO4J	Fine
0.18%	NO3I + NO3J	Fine

Table 12: EPA health risk for daily exposure to total $PM_{2.5}$ concentrations between C_{low} and C_{high} ug/m^3

C_{low}	C_{high}	I_{low}	I_{high}	**Category**	**Color Code**
0	15.4	0	50	Good	Green
15.5	40.4	51	100	Moderate	Yellow
40.5	65.4	101	150	Unhealthy for Sensitive Groups	Orange
65.5	150.4	151	200	Unhealthy	Red
150.5	250.4	201	300	Very Unhealthy	Purple
250.5	350.4	301	400	Hazardous	Dark Red/Brown
350.5	500.4	401	500	Hazardous	Dark Red/Brown

Table 13: Estimated CMAQ linear model for standard deviation of the error as a function of CMAQ estimated ***Tau,*** based on 40-case days with and without MODIS data-assimilation: CMAQ_***Tau***_**error**$_{standard\_deviation}$ ≈ INTERCEPT + SLOPE * (***Tau***_CMAQ)

CMAQ Subdomain and 40-day Run	SLOPE	Intercept
East baseline	0.09743	0.21986
East assimilated	0.00360	0.18484
West baseline	0.22793	0.15535
West assimilated	0.50498	0.04393

Figure 1. Comparison of baseline (non-assimilating) CMAQ total AOD calculated using the (a) original IMPROVE method and (b) the revised-IMPROVE method against all viable surface AERONET observations for the 2002 annual VISTAS simulation.

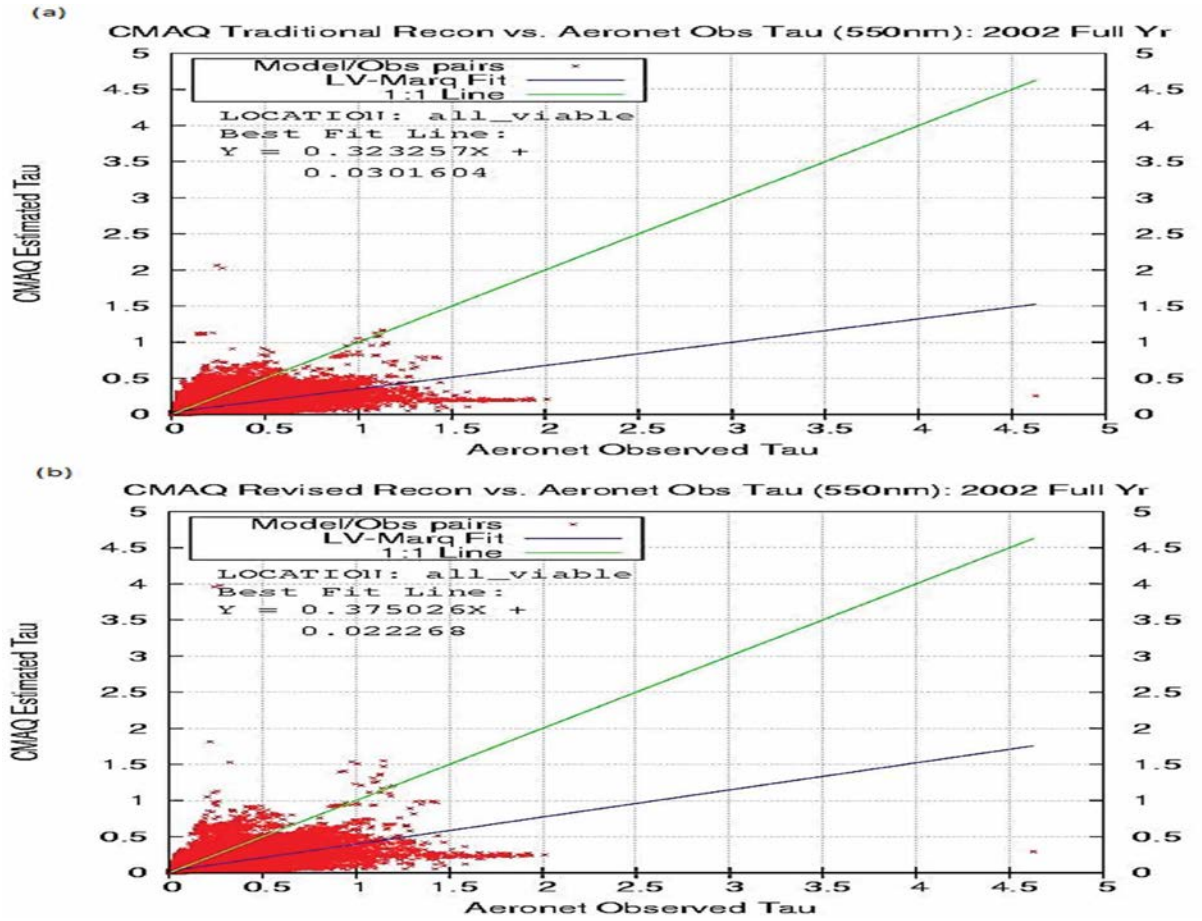

Figure 2. MODIS data valid between 1815 GMT and 1845 GMT overlaid as diamonds against the CMAQ 36km CONUS grid depicting a daily composite of all valid MODIS retrievals "super-obbed" into their respective 36km CMAQ grid cells for an operational run made on July 16, 2015. Grid cells in white contained no valid MODIS observations across the entire day.

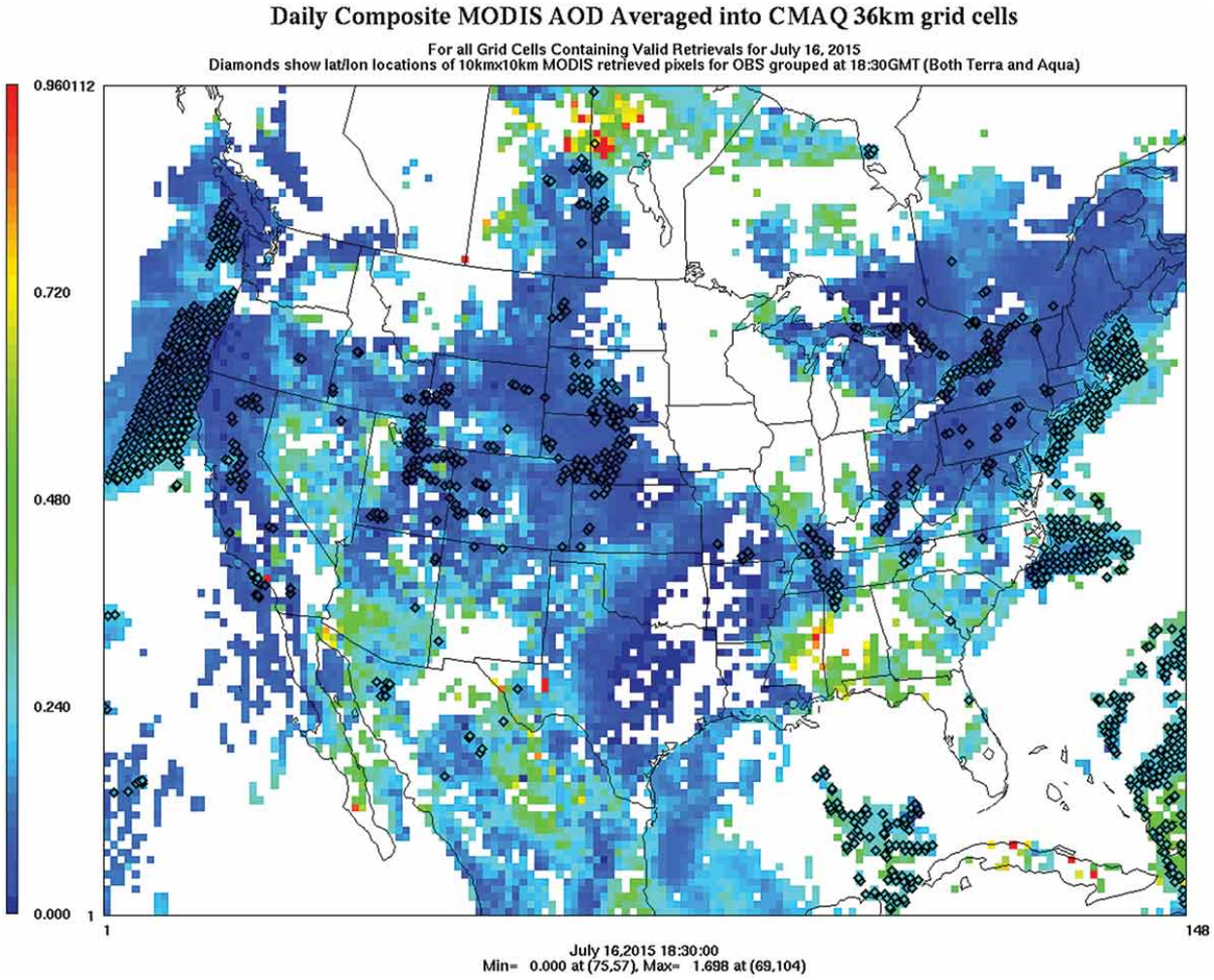

Figure 3. Aggregated result of MODIS/Terra AOD data assimilation in CMAQ across 40 selected 2002 case days for the entire CONUS measured against surface AERONET AOD observations: (a) The baseline, non-assimilated result; (b) the assimilated result. Significant improvement in the slope of the best fit line is noted.

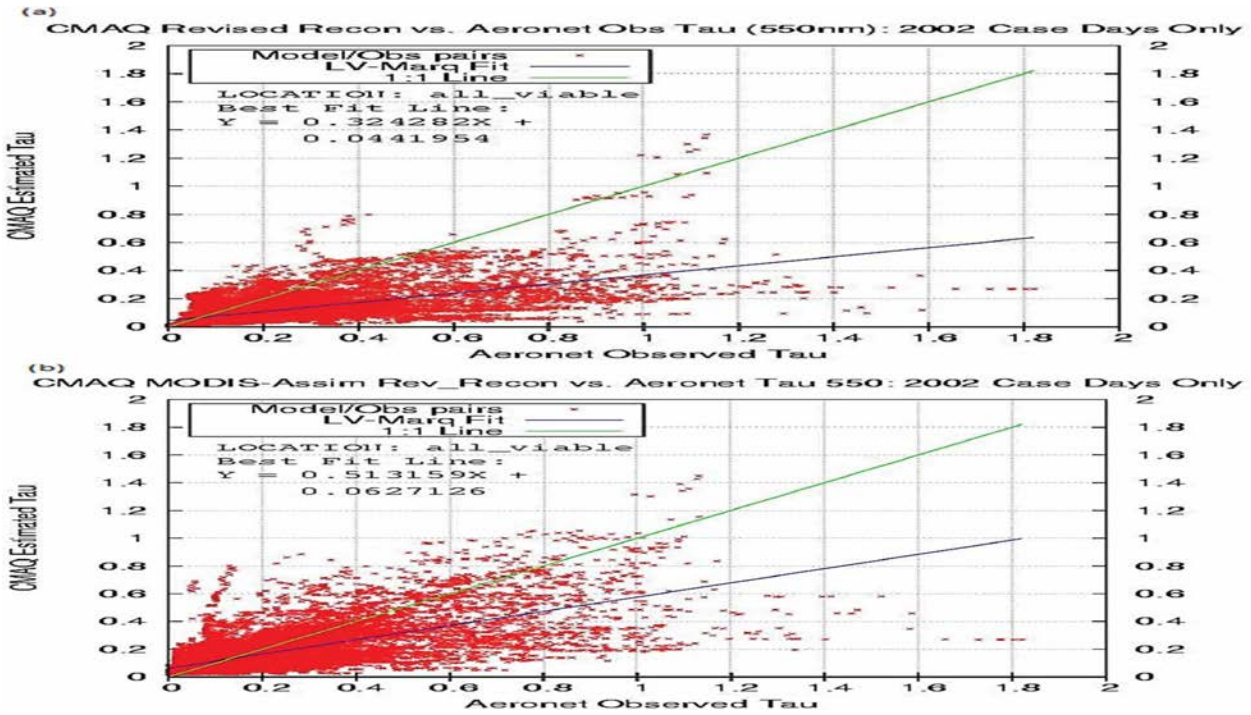

Figure 4. Results for eastern US total $PM_{2.5}$ mass from the FRM network (a and b, top row) and the IMPROVE network (c and d, bottom row). Baseline VISTAS results are shown in the left-hand column (a and c), CMAQ-data-assimilating results are shown in the right-hand column (b and d). Daily average (24-hour) values are paired to make the comparison.